

Classification of Al-Hammar Marshes Satellite Images in Iraq using Artificial Neural Network Based on Coding Representation

¹Ashraf S. Abdulla, ¹Bushra Q. Al-Abudi and ²Mohammed S. Mahdi

¹Department of Astronomy and Space, College of Science, Baghdad University, Baghdad, Iraq

²Department of Computer Science, College of Science, Al-Nahrain University, Baghdad, Iraq

Key words: Classification, Landsat satellite images, back propagation artificial neural network, Al-Hammar marshes, MATLAB

Abstract: In this study, Landsat satellite images of hammar marshes and surrounding district in (Dhi Qar) province in the South of Iraq are classified by Back Propagation Artificial Neural Network (BPANN) for years 1991, 2000, 2015 and 2017. Firstly, Principle Components Analysis (PCA) is applied on six bands of these satellite images using MATLAB programming and the information of all six bands concentrated in first three principle component and then blended to form integrated image. Then the integrated image is classified using proposed method (BPANN) method based on encoding elements. In this proposed method (BPANN) there are two paths are considered training and classification. The estimated coded descriptors are input to the training and classification phases of the ANN. It is intended to prove that the encoding capabilities can lead to improve the classification accuracy. The training is useful to indicate the basic information about image classes that represented by some specified statistical features while the classification uses the same features to produce the final classification results in terms of training results. Results evaluation is carried out for validation purpose. Then, quantitative and qualitative analysis is estimated to evaluate the performance of the proposed classification method. The artificial neural network showed valued ability for classifying satellite images.

Corresponding Author:

Mohammed S. Mahdi

Department of Computer Science, College of Science,
Al-Nahrain University, Baghdad, Iraq

Page No.: 241-249

Volume: 10, Issue 11, 2019

ISSN: 1682-3915

Asian Journal of Information Technology

Copy Right: Medwell Publications

INTRODUCTION

One of the main purposes of satellite remote sensing is to interpret the observed data and classify features. In addition to the approach of photo interpretation, quantitative analysis which uses computer to label each pixel to particular spectral classes (called classification) is commonly used. Quantitative analysis can perform true multispectral analysis, make use of all the available brightness levels and obtain high quantitative accuracy (Campbell and Wynne, 2011). The two general classification methods which are used most often are: supervised and unsupervised classification, the main difference between the two methods is that the classification observer built on real information about geographical phenomena given the current computer

while the rating unattended done in accordance with mathematical equations define gatherings clusters and thus classification categories, according to the relationship between the numeric values of the ranges of image (Gustavo *et al.*, 2011). In this study, the satellite image classification is done using artificial neural networks which is applied in many applications such as automotive, aerospace, banking, medical, robotics, electronic and transportation. Another application of NN is in remote sensing for classification of images. Many methods of classification have been already proposed. Pacifici *et al.* (2009) used very high-resolution panchromatic images from quick bird of four different urban environments: Las Vegas (USA), Rome (Italy), Washington DC (USA) and San Francisco (USA). The proposed method is based on the analysis of first and second-order multi-scale textural

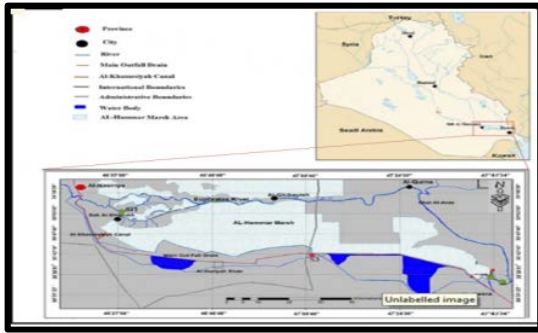


Fig. 1: Location of study area within Iraq

features extracted from panchromatic data. Neural network pruning and saliency measurements made it possible to determine the most important textural features for sub-metric spatial resolution imagery of urban scenes. Eleyan and Demirel, (2011) used two methods to extract feature vectors using (GLCM) for face classification. The first method extracts the well-known Haralick features from the GLCM and the second method directly uses GLCM by converting the matrix into a vector that can be used in the classification process. Sahin and Erol (2017) developed and applied a Neural Network (NN) approach and an Adaptive Neuron-Fuzzy Inference System (ANFIS) Model for forecasting the attendance rates at soccer games. The models were designed based on the characteristics of the problem. Training data was used for training the models and the testing data was used for evaluating the performance of the forecasting models.

Study area: The area under investigation is Al-Hammar marsh. Iraqi marshes are important as they have economic, social and biodiversity value. The marshes suffered from many changes from 1980 to this time because of many dry areas in the end century. These drying operations have resulted in drastic changes in the marsh environment which is still suffering until today. After 2003 the marshes were refilled but degradation in water quality and ecosystem still endures. Al-Hammar marshes are one of the three biggest marshes located in the southern parts of Iraq. It is situated to the south of the Euphrates river and is approximately bounded by the following coordinates (longitude 30°45'-30°59'N, latitude 46°25'-47°15'E") and has an area ranging from 2800 km² of contiguous permanent marsh to 4500 km² during flooding periods. In 2016 the UNESCO inscribed property is the fifth site from Iraq to be included in the world heritage list, after Ashur, Hatra, Samarra Archeological city and Erbil Citadel. Figure 1 shows the original map of Iraq and the location of the study area within Iraq. Four types of satellite images were consulted during the work, Landsat-5 (TM) satellite image (5/6/1991 and 14/6/1991), Landsat-7 (ETM+) satellite image (6/6/2000 and 13/6/2000) and Landsat-8

(16/6/2015 and 23/6/2015) and (OLI) satellite image (5/6/2017 and 12/6/2017) with (Path/Row166/39) and (Path/Row167/39). All four images are geometrically projected using Universal Transverse Mercator (UTM) coordinate system and World Geodetic System 1984 (WGS84) zone 38 and obtained from the USGS Earth explorer database.

MATERIALS AND METHODS

Software programming ENVI is used for preprocessing satellite images of Al-Hammar marshes (geometric, atmospheric and radiometric correction), mosaic two scenes and clipping the interest region. Then Principle Components Analysis (PCA) is applied on six bands of these satellite images using MATLAB. In this research, we did not select the first principal component (PC1) as usual in this transform but the most information PCs components are chosen, the computed variance (σ^2) can be measured the appearance of details in each PC band. For each year, the three components of the most variances are regarded as the three adopted components of the satellite image. The PC_{final} image produced depending on using the first three PCs image that contain the most details to create one PC_{final} image. To determine the contribution weight of each PC component to produce the PC_{final} image, we divided the variance of each component on the total variance of first three PCs using Eq. 1-2. A maximum weight will be specified to the first PC component denoted as w_1 while less weight for the second PC as w_2 and then the least weight is assigned for the third PC and denoted as w_3 :

$$w_i = \frac{\sigma_i^2}{\sum_{i=1}^3 \sigma_i^2} \quad (1)$$

$$PC_{final} = w_1 \times PC_1 + w_2 \times PC_2 + w_3 \times PC_3 \quad (2)$$

Then PC_{final} image is classified using proposed method Back Propagation Artificial Neural Network (BPANN) as follows:

Satellite Image Classification using proposed method BPANN: The proposed satellite image classification consists of five primary steps followed by two phases: training and classification as shown in Fig. 2. More details related to each step are given in the following sections.

Image encoding: Image encoding stage is used to change the representation of image regions with others that are more appreciable. The encoding is a computer procedure based on partitioning the image into small parts, each possesses a specific detail which can be processed to estimate the corresponding code that describes the current image region. Therefore, the test image is partitioned into overlapped blocks; each block describes the behavior of the pixel lies

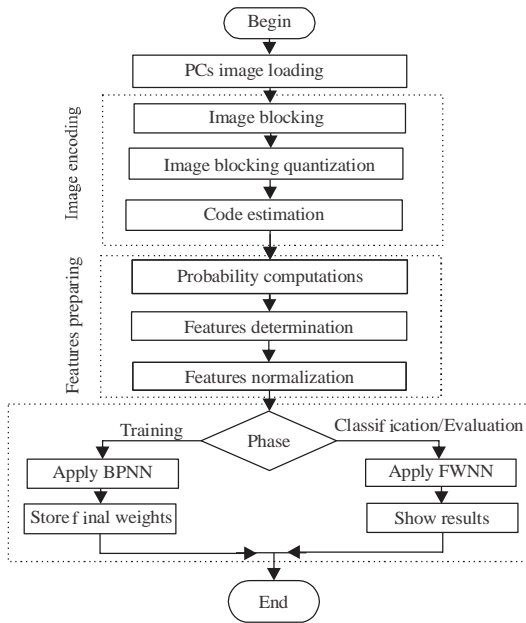


Fig. 2: Block diagram of the proposed classification method BPANN

Table 1: The three equally range intervals

| Range title | Grey ranges |
|-------------|-------------|
| R1 | 0-84 |
| R2 | 85-169 |
| R3 | 170-255 |

in the center of the block. Then, a code array is estimated for each block to reflect the specific content of the image in that region. The following subsections explain more details about the three steps that employed to implement the adopted image encoding stage:

Image blocking: Image blocking is applied on the gray image (G_s) to be partitioned into a specific number (N_B) of squared blocks in which the size of each block is $w_s \times w_s$. Each block is like a window moving along the vertical and horizontal axes of the image with a shifting distance is equal to one pixel. Such that, N_B is equal to the size of the image minus double w_s . In the present step, each pixel in the image that can be enclosed in $w_s \times w_s$ window will be represented by its corresponding image block ($B_{i,j}$) where i and j are pointers refer to the position of the current block in the image. The maximum value of i is equal to the width (W) of the image minus w_s , whereas the maximum value of j is equal to the height (H) of the image minus w_s . Practically, it is found that the best value of N_B is three which gave most acceptable results. These spectral ranges are determined to be equal and extended along the grey scale, these useful ranges are given in Table 1. Also, the useful size (w_s) of the opened window is 3×3 pixels in which the considered pixel lies at the center of the window.

| | | |
|-----|-----|-----|
| 36 | 143 | 78 |
| 237 | 112 | 82 |
| 92 | 41 | 196 |

| | | |
|---|---|---|
| 0 | 1 | 0 |
| 2 | 1 | 0 |
| 1 | 0 | 2 |

Fig. 3(a-b): Quantized block corresponding to the original one

Block quantization: The quantization process is applied to each image block to determine the signature of intensity variation within the current pixel. The image block quantization is carried out by the following procedure: for a given block B_{ij} , one can assume that the number of grey levels is (R_N). For example if the number of ranges is three, then $R_N = 0, 1$ and 2 . Such that N_B is one dimensional array in which N_0 is the number of pixels lies in the first grey range (R_0), N_1 is the number of pixels lies in the second grey range (R_1) and N_2 is the number of pixels lies in the second grey range (R_2). Then, a specific two dimensional quantized array $Q(i, j)$ with same size of given block is created, the elements of this array is pointer refers to the range that the pixel of the original block lie on, i.e., the elements may be one of the values: 0, 1 and 2 in corresponding to the ranges R_1, R_2 and R_3 . Figure 3a shows the quantized block corresponding to the original one in such example, the three ranges are assumed to be equal with increasing amount of about 86 grey level such that the first range R_0 is 0-84, the second range R_1 is 85-169, the third range R_2 is 170-255. The pixel lies in between the minimum and maximum value of each range is replaced by its range pointer in the quantized block as shown in Fig. 3b. The practical tests show that the use of the larger block size (w_s) leads to confuse the encoding results it is found that the consideration of 5×5 pixel block size affects the results of code arrays due to less recognition may appear for more detailed image blocks. In other words, the larger block size may lead to include more pixels belonging to other classes which make the tag of the code array to be larger and more similar to other blocks that belong to a different class.

Code estimation: For each given image block, the produced code is two dimensional array representing the intensity signature of that block in the test image. This code array is determined by computing the number of transitions between successive quantized grey levels in the same image block. Therefore, the computing transition is a two dimensional array $C(m, n)$ where both m and n are equal to R_N . Each element in $C(m, n)$ is the number of right horizontal transitions between pixel pointers in $Q(i, j)$ that corresponds to the location m, n . Implies, $C(0, 0)$ is equal to the number of existing two horizontally adjacent pixels each has pointer value of 0 while $C(0, 1)$ is equal to the number of existing two horizontally

adjacent pixels in which the pointer value of the first pixel is 0 and the pointer value of the second is 1. As a result, the code array represents the frequency of appearing any two grey levels that are adjacent in the current block.

Features extraction: Features are extracted from the code array to describe the behavior of each pixel in the image. This process is a computer procedure based on a mathematical approach enables to recognize current pixel automatically by extracting its textural features. The probability computation is a primary stage due to the statistical features is depending on the probability in their computations. The following subsections explain the two steps of the feature extraction stage:

Probability computations: The probability computation requires considering a window of size ($w_s \times w_s$) for each pixel to estimate the frequency that leads to determine probability $P(i, j)$ of the current pixel. Such that, the code array $C(i, j)$ is representing a recognizable signature for each pixel in the image which can be used to compute the probability of the pixel appearance in the image block. Since, transition array is computed as the frequency of appearing each quantized pixel in the considered window, the probability $P(i, j)$ of current pixel is produced by normalizing the summation of $C(i, j)$ with its transposed array $C^T(i, j)$, the summation is used to credit the summitry of the produced array. The normalization is implemented by dividing each element in $P(i, j)$ by the total numerical sum (S_T) of all elements in $P(i, j)$ Eq. 3 which is used to credit the produced values of $P(i, j)$ are in between 0-1.

$$P(i, j) = \frac{C(i, j) + C^T(i, j)}{S_T} \quad (3)$$

The description of each pixel in the image based on using its 3×3 code array such description depends on determining the probability P_{ij} of each code array C_{ij} of the quantized image block Q_{ij} that belong to the pixel G_{xy} .

Features computation: The features want to be extracted are depending on the probability $P(i, j)$ of each pixel. The computations of such features are related to the details found in the considered image region which leads to determine a specific probability of pixel appearance for each pixel in the image and then specify distinct features for this pixel. The seven computed features are stored in a features vector f_i to be employed in the next stage. The mean (μ_i) and variance (σ^2) of the resulted values of the adopted eleven features for satellite image sample for year 1991.

Features preparation: Features preparation stage is a modification process carried out on the features vectors to make them more reliable for the classification task. In this stage, each feature in the features vector is regarded as a descriptor which must be examined for inspection of its behavior if it is stable and gives acceptable results of discrimination or not. Furthermore, this stage considers the collective behavior of all descriptors together and searches to exclude the descriptor that inverts its behavior when it integrates with others. Therefore, features selection is adopted to consider each descriptor in terms of different subjects related to their values, ranges and responses. Then, the succeeded descriptors are modified by using the normalization to be useful in the classification task. More explanations about features preparation stage are given in the following subsections:

Features selection: The computed features vector is varying according to the great variations of fine details found in the satellite image. The interfering of windows needed to estimate the features vector of adjacent pixels is lead to interfere the ranges of computed feature values. Therefore, it is necessary to check the discrimination between the ranges of the used features that belong to different regions in same image. The problem when considering many feature descriptors is that there is less scattering for each descriptor and closer centers of these descriptors. Such problem can be exceeded by employing the feature selection to credit the trust ranges of all used feature descriptors.

Features normalization: The used features are resulted in different ranges it is intended to make its values extended between the range (-1 to 1). This process requires using a linear fitting for modeling the relation between the behaviors of each feature (F_s) and the new intended behavior (F_N) of normalized features. The determination of minimum (Min) and maximum (Max) values of each feature that corresponding to a minimum (-1) and maximum (1) values of the normalized range enable to compute the normalized feature value (F_N) using the linear relationship given in Eq. 4:

$$F_N = 2 \times \frac{F_s - \text{Min}}{(\text{Max} - \text{Min})} - 1 \quad (4)$$

Training phase: The application of ANN need to a previous knowledge about the data that deal with. The previous knowledge comes from training ANN to know more about the materials data. The supervised training requires existence a confident classified image to indicate the class of each pixel. For the purpose of training, the classification information is stored in a codebook table to be compared with the simultaneous classification results

Table 2: Codeword of available classes

| Class | Codeword (C_{NC}) |
|-------|-----------------------|
| C1 | 00001 |
| C2 | 00010 |
| C3 | 00100 |
| C4 | 01000 |
| C5 | 10000 |

of the designed Back Propagation Artificial Neural Network (BPANN). The continuous comparison of the training results leads to back propagate the results and modify the weights of the designed ANN according to the true classification information found in the codebook table which enable to improve the training and achieving better classification results at each training loop. The way by which the codebook is constructed and how training the designed BPANN are explained in the following subsections:

Codebook estimation: The codebook is built depending on the confident classification information available for the same test image. For each pixel in the test image, the class is determined and stored in the codebook table. The first column of this table contains the class title of the pixel while the second column contained the codeword of the meant pixel. The codeword consists of five binary digits referring to one class as given in Table 2. Accordingly, the codebook is formulated as given in Table 2 in which the length of the first column is equal to the total number of pixels in the image. The existence of all pixels in the codebook table makes some redundancy in the information such that a redundancy removing procedure should be carried out to abstract the codebook table. The third column in the codebook table contains a set of the eleven adopted descriptive features that belong to the current pixel.

BPANN design: The use of back propagation training method for supervised learning is the best one that can achieve accepted results. The structure of designing ANN based on back propagation algorithm consists of three layers: Input layer (I), Hidden layer (H) and Output layer (O). In addition to the base of each layer, there are eight nodes are found in the first input layer, each node represents one attribute of the input data. The base input node is denoted as F_0 while other seven input nodes are denoted as: $F_1, F_2, F_3, \dots, F_{N_F}$. The output layer contains a number of output nodes is equal to the number of classes found in the image (e.g., five). The output nodes are denoted as: $R_1, R_2, R_3, R_4, \dots, R_{N_C}$. Whereas, the hidden layer contains eight nodes; one is the base that denoted as: H_0 and the other seven are determined to be equal the median value between the number of nodes of both the input and output layers. These hidden nodes are denoted as: $H_1, H_2, H_3, \dots, H_7$. Each node in one layer is connected to all nodes in the next layer there is a determined weight

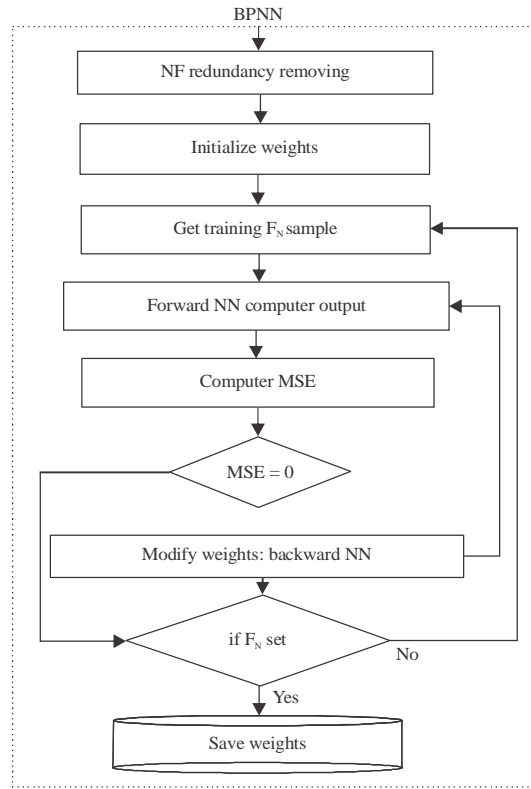


Fig. 4: Sequential stages of training phase

is specified for each connection are denoted according to the serial of the connected nodes in frequent two layers. Such that the symbol $w_{i,j}^k$ denotes to the weight of the connection between the i th node in the k th layer with the j th one in the next layer. In which $i = 0, 1, 2, \dots, N_F; j = 0, 1, 2, \dots, N_C$ and $k = 1, 2$ where N_C is the number of known classes in the reference classified image and N_F is the number of used descriptive features. The following subsections explain more details about the forward and backward actions of the designed BPANN. Figure 4 shows the sequential steps of the training phase.

Forward BPANN: The work flow of training the designed BPANN is starting with input the calibrated features (F_N) of first pixel in the classified image to the input layer. Each feature is assigned to one input node to be its value. The initial weights $w_{i,j}^k$ are chosen randomly between the range 0-1 to be used for activating the input nodes and resulting normalized values using the sigmoid function. In particular, the value of the j th node in the hidden layer (H_j) is determined by computing the result when loading the value (y_j) to the sigmoid function where y_j is computed by summing the multiplications of i th input nodes values (F_{N_i}) with their weights $w_{i,j}^2$. Whereas the activation of the output layer is carried out by the same

manner as follows; The value of the j th node in the output layer (R_j) is determined by computing the result when loading the value (y_j) to the sigmoid function where y_j is computed by summing the multiplications of i th hidden nodes values (H_i) with their weights $w_{i,j}^2$. The result of each output node is a binary number. As a result, the result of the output layer is a binary code consists of five digits each is resulting from one output node. This result is compared with the ones saved in the codebook that belonging to the current pixel using a specific fidelity criterion; the most useful fidelity is the similarity measure that can indicate the similarity between two wordcodes using the relation of the Mean Squared Error (MSE) given by the following equation:

$$E_h = \sum_{j=1}^{N_c} |C_j - R_j| \quad (5)$$

$$MSE = \frac{E_h}{N_c} \quad (6)$$

where, C_j denotes the computed output of the node j , R_j denotes the real output of the node j from the codebook that belonging to the current pixel if the comparison result is identified ($MSE \leq 0.0001$) then the designed BPANN leaves the current pixel and get the next one with initial weights are equal to the final ones resulted from the current pixel, otherwise the designed BPANN goes to modify the weights of the connection between all the nodes in all layers using backward BPANN and then repeat the implementation of forward BPANN in terms of the new modified weights.

Backward BPANN: The backward action of BPANN has happened when the similarity measure between the result of the output layer and the codeword in the codebook table is not identified. In such case the direction of computations is carried out in backward these computations are related to modifying the weights of connecting each node in a specific layer with others in another layer. The process is starting by modifying the weights $w_{i,j}^2$ that connecting the nodes of the output layer with that of the hidden layer), the modification requires modify the values of the nodes in the output layer in such case, the modification of the weights $w_{i,j}^2$ includes adding a determined amount to weights is equal to the result of output node R_j multiplied by both its error δ_j^1 and the learning rate η . Also, the modification of the weights $w_{i,j}^1$ requires first modifying the values of the hidden layer nodes. By the same manner compute error δ_j^2 , the values (H_i) of the hidden layer nodes are modified which leads to modify the weights $w_{i,j}^1$ between the hidden and input layers using hidden layer error ratio δ_j^2 , then modify $w_{i,j}^1$.

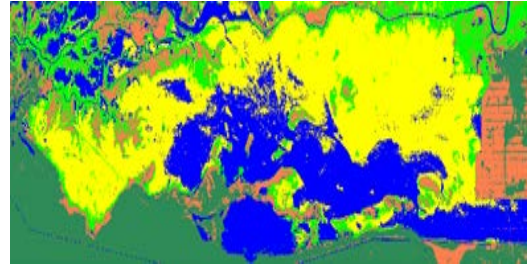


Fig. 5: Classification result of reference satellite image, that classified by ENVI for the year 1991

Table 3: Classification results of reference satellite image for year 1991

| Classes | Colors | Name of class | P _c % |
|-------------|--------|---------------|------------------|
| Class one | Brown | Wetland | 8.8 |
| Class two | Blue | Water | 26.7 |
| Class three | Green | Agri land | 10.2 |
| Class four | Yellow | Grass | 27.6 |
| Class five | Green | Desert | 26.7 |
| Total sum | | | 100 |

The process of back propagation is continuing for many times each time the back propagation is carried out, the results of the output layer converge to the real ones found in the codebook. More results enhancement is yields with more weights modifications. This situation is continuing till reaching identification state for each pixel in the image. The resulted final weights are saved in two three dimensional array $W_{h,j,i}^k$ $k = 1, 2$ for two layers to represent the experience gained by the training phase. The training of proposed BPANN is implemented on the data extracted from reference image shown in Fig. 5 that classified using ENVI software programming for year 1991, Table 3 presents statistical information of reference image, these information is percent (P_c) for each class in the reference image.

The selection of just useful features for training the BPANN helps to obtain the ideal weights that want to be employed in classifying the images that not previously classified. In the training implementation, the number of iterations was determined to be 1000 for each training process of one pixel or till reaching the MSE into 0.001, in which the learning ratio was 0.5. These restriction values gave the most confident results where the weights begins with random initial values and soon reached true values whatever the initial value is it is found that the weight is biased towards its true value with 1000 training iterations it is going away from their true values in the event of an increase training iterations. Also it is noticeable that the weights settle at certain values at the last iterations and there is no change may occur on them with increasing the training iterations. In such case, the MSE that computed between the result of BPANN and the true one in the codebook table becomes smaller at each

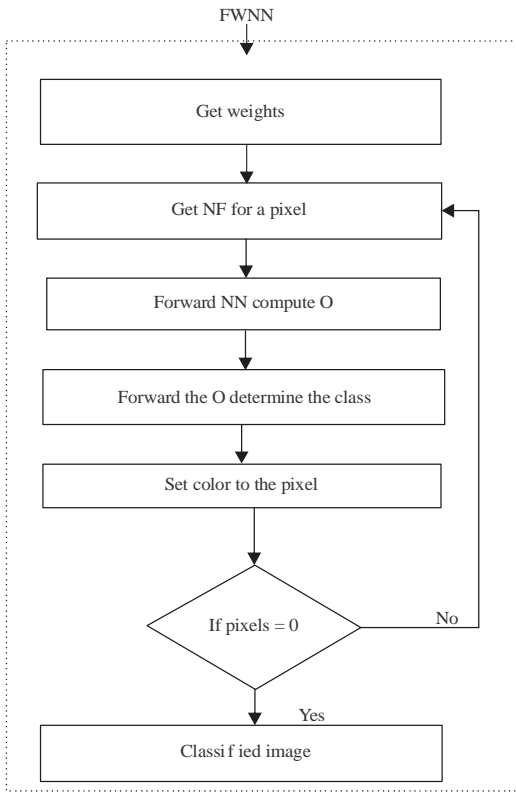


Fig. 6: Stages of the classification phase designed BPANN

training iteration till reaching the ideal values of the weights this result ensures that the number of iteration and learning ratio was sufficient to obtain acceptable classification results, the time spent in the training process on all data after deleting duplicate data and for the purpose of reaching the best weights is 2438 sec mean 40.6333 min, it is possible to reduce the training time by selecting training areas from the reference image containing all five categories and deleting duplicates there of.

Classification phase: The classification phase uses the same structure of the designed BPANN as in the training phase. Figure 6 shows the sequential stages of the classification phase of the designed BPANN. The computation in such case is done one time in forward direction using the final weights resulted from the training phase, the nodes of each layer are activated using the sigmoid function. The final classification result is the desired output of the output layer.

In order to evaluate the classification performance, the results are compared with the reference classified image. The comparison result includes some measures indicated the amount of convergence of the classified image from the reference one. These measures are: the number of pixels (N_{p1}) in each class in the resulted

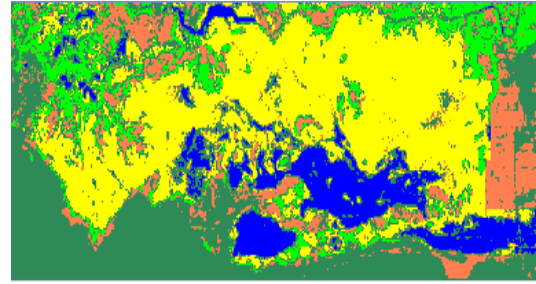


Fig. 7: Classification result of satellite image for Al-Hammar marshes for year 1991 using proposed BPANN

Table 4: Classification statistical measures of satellite image for year 1991

| Class | N_{p1} | N_{p2} | T_c | $P_{TC}\%$ |
|------------|----------|----------|--------|------------|
| Wet land | 22356 | 22356 | 22356 | 8.8 |
| Water | 67829 | 67829 | 67829 | 26.6 |
| Agri. Land | 26166 | 26166 | 26166 | 10.3 |
| Grass | 70116 | 70116 | 70116 | 27.6 |
| Desert | 67576 | 67576 | 67576 | 26.7 |
| Total sum | 254043 | 254043 | 254043 | 100% |

classified image, the number of pixels (N_{p2}) in each class in reference classified image, the number of true classified pixels (T_c) in classified image in comparison with the reference classified image, the classification percent of true classified pixels (P_{TC}) in classified image, the number of false classified pixels (F_c) in classified image comparison with the reference classified image and the classification percent (P_{FC}) of false classified pixels in the classified image. The resulted weights were firstly tested by classifying satellite image of same period of reference image (i.e., 1991). Figure 7 displays the classification result of the satellite image of 1991 period that used in the proposed BPANN training while Table 4 shows its resulted statistical measures of the classification process. It is shown that the proposed BPANN could to classify all the image pixels efficiently it has relatively achieved full discrimination results where the final classification score was 100% which indicates that there is no pixel in the given image is left without classification or false classified. Figures 8 and 9 shows the classification result of satellite images of the periods 2000, 2015 and 2017 while Table 5-7 lists the classification measures of these results.

It is shown that the classification percent are 100% for year 1991, 97.6% for the year 2000, 95.4% for year 2015 and 83.7% for year 2017. These results are achieved using same training information obtained from the image of period 1991. The mis-classification percent are 0, 13, 4 and 7% frequently for the same used years. The full classification percent of year 1991 ensure correct behavior of the proposed BPANN classification method while the mis-classification found in the classification results for other used images are due to the change occurred in the land cover. These results are subject to change depending

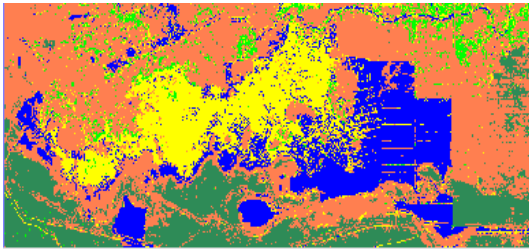


Fig. 8: Classification result of used satellite image for the period 2015 using proposed BPANN

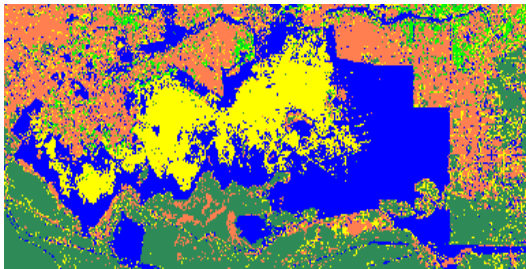


Fig. 9: Classification result of used satellite image for the period 2017 using proposed BPANN

Table 5: Classification statistical measures of satellite image for year 2000

| Class | N_{P1} | N_{P2} | T_C | $P_{TC}\%$ |
|------------|----------|----------|--------|------------|
| Wet land | 22356 | 22547 | 22356 | 8.8 |
| Water | 67829 | 62284 | 62287 | 24.5 |
| Agri. land | 26166 | 25981 | 25981 | 10.2 |
| Grass | 70116 | 69746 | 69746 | 27.5 |
| Desert | 67576 | 73485 | 67576 | 26.6 |
| Total sum | 254043 | 254043 | 247946 | 97.6% |

Table 6: Classification statistical measures of satellite image for year 2015

| Class | N_{P1} | N_{P2} | T_C | $P_{TC}\%$ |
|------------|----------|----------|--------|------------|
| Wet land | 22356 | 19294 | 19294 | 7.6 |
| Water | 67829 | 63386 | 63386 | 24.9 |
| Agri. land | 26166 | 29939 | 26166 | 10.3 |
| Grass | 70116 | 65935 | 65935 | 25.9 |
| Desert | 67576 | 75489 | 67576 | 26.7 |
| Total sum | 254043 | 254043 | 242357 | 95.4% |

Table 7: Classification statistical measures of satellite image for year 2017

| Class | N_{P1} | N_{P2} | T_C | $P_{TC}\%$ |
|------------|----------|----------|--------|------------|
| Wet land | 22356 | 17529 | 17529 | 6.9 |
| Water | 67829 | 82793 | 67829 | 26.7 |
| Agri. Land | 26166 | 13476 | 13476 | 5.3 |
| Grass | 70116 | 46224 | 46224 | 18.2 |
| Desert | 67576 | 94021 | 67576 | 26.6 |
| Total sum | 254043 | 254043 | 212634 | 83.7% |

on the training data used in the reference image and through research and experimentation it is possible to reduce the training time by selecting the training areas of the image, provided that it contains all five categories and result of classification relatively close to the previously mentioned, the classification time is very short as it does not take parts of a second for all kinds of images.



Fig. 10: The regular area in Al-Hammar marshes



Fig. 11(a-b): Some photos taken during the visit to the marsh lands on 17/1/2018

RESULTS AND DISCUSSION

Felid work: During this researcher, we encountered some problems for example: some region in satellite image have regular arrange while in fact there are no arranged region in marshes as shown in Fig. 10.

So, it was necessary to visit the marsh lands to determine the cause of these problems. The visit was made at 17/1/2018 to the province of Dhi-Qar in the South of Iraq and specifically, to the Al-Hammar marshes. Coordinate of different classification area have been identified using a Global Position System (GPS) as shown in Fig. 11 which shown some photos taken during the visit to the marsh lands. By comparing the coordinate extracts

in satellite image with the ground coordinates by GPS, we were able to get answers for some things, firstly, there are arranged regional areas created by the previous regime, before 2003 and it was distributed as land pieces for specific people. Secondly, through interviewing with a few people, we have concluded that most of the moisture lands contain clay soil.

CONCLUSION

Throughout the implementation of the present work, a number of conclusions have been achieved based on the practical results. The following statements summarize the most important ones: the training results are greatly affected by the quality and quantity of the used data set, this effect was noticed as passive once and active in another time. The artificial neural network showed valued ability for classifying satellite images. The use of supervised training the artificial neural network make the present method to be restricted in providing pre-classified image as data reference, the classification results are depending on the quality of reference image classification.

The use of the seven textural features enables to describe the fine details of the test image. The use of scatter analysis method for features selection leads to

eliminate the un useful qualities throughout the training phase and reduces the computation time significantly this also leads absolutely to enhance the classification results. The use encoded features as inputs to the proposed BPANN was actually led to improve the classification results.

REFERENCES

- Campbell, J.B. and R.H. Wynne, 2011. Introduction to Remote Sensing. 5th Edn., Guilford Press, New York, USA., ISBN:978-1-60918-176-5, Pages: 684.
- Eleyan, A. and H. Demirel, 2011. Co-occurrence matrix and its statistical features as a new approach for face recognition Turk. J. Electr. Eng. Comput. Sci., 19: 97-107.
- Gustavo, C.V., T. Devis, L.G. Chova, J. Sandra and J. Malio, 2011. Remote Sensing Image Processing. 4th Edn., Morgan & Claypool Publishers, San Rafael, California, USA., ISBN:9781608458196, Pages: 176.
- Pacifici, F., M. Chini and W.J. Emery, 2009. Remote Sensing of Environment. Elsevier, America, USA.,
- Sahin, M. and R. Erol, 2017. A comparative study of neural networks and anfis for forecasting attendance rate of soccer games. Math. Comput. Appl., 22: 1-12.